JACS
JOURNAL OF THE AMERICAN CHEMICAL SOCIETY
Communication
pubs.acs.org/JACS

Photoelectron Spectra of Aqueous Solutions from First Principles

Alex P. Gaiduk,[†] Marco Govoni,[‡,†] Robert Seidel,[§] Jonathan H. Skone,[†] Bernd Winter,[§] and Giulia Galli*[,†,‡]

[†]Institute for Molecular Engineering, The University of Chicago, Chicago, Illinois 60637, United States
[‡]Materials Science Division, Argonne National Laboratory, Argonne, Illinois 60439, United States
[§]Methods for Material Development, Helmholtz-Zentrum Berlin für Materialien und Energie, D-12489 Berlin, Germany

Supporting Information

ABSTRACT: We present a combined computational and experimental study of the photoelectron spectrum of a simple aqueous solution of NaCl. Measurements were conducted on microjets, and first-principles calculations were performed using hybrid functionals and many-body perturbation theory at the G_0W_0 level, starting with wave functions computed in ab initio molecular dynamics simulations. We show excellent agreement between theory and experiments for the positions of both the solute and solvent excitation energies on an absolute energy scale and for peak intensities. The best comparison was obtained using wave functions obtained with dielectric-dependent self-consistent and range-separated hybrid functionals. Our computational protocol opens the way to accurate, predictive calculations of the electronic properties of electrolytes, of interest to a variety of energy problems.

Computational engineering of systems for new energy sources,[1−3] for example, materials to be employed in photoelectrochemical cells for water splitting, requires the availability of methods to accurately determine the ionization potentials (IP) and electron affinities (EA) of electrodes and electrolytes, including solutions of salts. The lowest IP and EA are related, for example, to the standard electrode potential of a material.[4] The electronic properties of salt solutions also play a central role in several processes of interest in biochemistry and atmospheric science.[5,6]

Recent experimental and theoretical developments have allowed one to probe the electronic structure of solutions. In particular, it has become possible to extend photoelectron (PE) spectroscopy[7,8] to liquids, thanks to the development of microjet techniques,[7,9,10] and to accurately determine the positions of the energy levels of liquid water[11] and of several simple aqueous solutions.[12−17] Theoretical methods have also become available, and several interesting studies of the valence PE spectra of simple aqueous solutions of Cl^-,[12,18−21] OH^-,[14,22,23] and other atomic and molecular ions[14,24−26] have appeared in the literature, which were performed using generalized-gradient approximations (GGAs) to density-functional theory (DFT). However, the results of these investigations were not completely satisfactory as often GGAs do not accurately reproduce the energy difference between single-particle states of the solute and the solvent;[18,27] moreover, these approximations yield absolute positions of peaks in the energy spectrum in poor agreement with experiment.[28]

Hybrid functionals contain a fraction of the exact exchange, which reduces the self-interaction error present in GGAs. In general, the use of hybrids improves the positions of the energy levels compared to GGAs. For example, the PBE0 approximation,[29,30] containing 25% of exact exchange, correctly predicts that the energy levels of solvated anions such as Cl^-,[18,20,21] OH^-,[23] and PhO^-[25] are located above the water valence band maximum, in qualitative agreement with experiments.[12,14,24] However, the computed anion level positions differ from the measured ones by as much as 1 eV. In addition, hybrid functionals used so far do not appear to reproduce the position of the energy levels of deep lying states such as that of the Na^+ cation.[20] Many-body perturbation theory (MBPT) calculations at the G_0W_0 level performed starting from GGA wave functions showed that MBPT has the potential of improving the PE spectra of solutions over DFT-based methods, although wave functions from GGAs did not seem to be a sufficiently good starting point for perturbative corrections.[18,23]

Here, we present a joint experimental and computational study of the PE spectrum of NaCl, using microject technique and first-principles calculations, respectively. Experiments were conducted on microjets with the same concentration of NaCl as investigated computationally. Our calculations were performed using a strategy that combined ab initio molecular dynamics (MD) simulations with accurate electronic structure calculations, beyond DFT. The latter were conducted using MBPT (at the G_0W_0 level) starting from wave functions computed with hybrid functionals. We report absolute positions of the energy levels with respect to vacuum and relative peak intensities which exhibit excellent agreement with experiment, and we show that the most accurate results are obtained using wave functions computed with self-consistent[31] and range-separated[32] hybrids.

The liquid-jet PE spectrum of a 1 M aqueous solution of NaCl measured using x-rays with energy of 200 eV is shown in Figure 1. It consists of several bands corresponding to the binding energies (BE) of valence electrons excited into vacuum. The bands are labeled according to the symmetry of single-particle states from which the emission occurs. Four peaks shown in Figure 1 ($2a_1$, $1b_2$, $3a_1$, and $1b_1$) are due to electrons ejected from water molecules, and two peaks (2p and 3p) correspond to electrons ejected from Na^+ and Cl^- ions, respectively. To describe processes occurring at aqueous interfaces with electrodes, it is necessary to accurately predict the absolute positions of the valence band maximum (VBM) of water and of ions close to $1b_1$ peak.

Received: January 8, 2016
Published: April 22, 2016

DOI: 10.1021/jacs.6b00225
J. Am. Chem. Soc. 2016, 138, 6912−6915

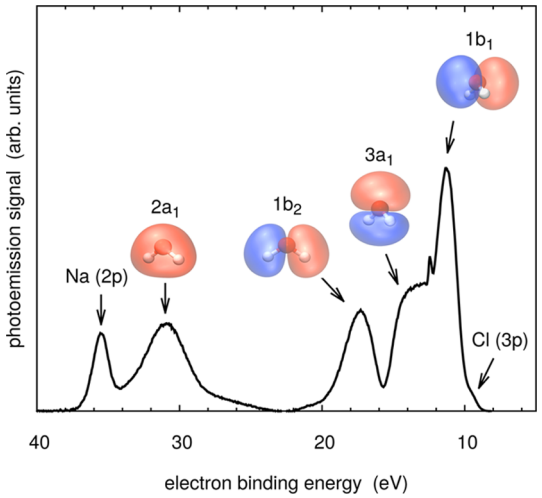

Figure 1. Experimental PE spectrum of a 1 M solution of NaCl and molecular orbitals of a single water molecule corresponding to specific bands in the spectrum. The background due to secondary electrons has been subtracted following ref 11. The sharp peak at 12.6 eV arises from ionization of the $1b_1$ orbital of gas-phase water.

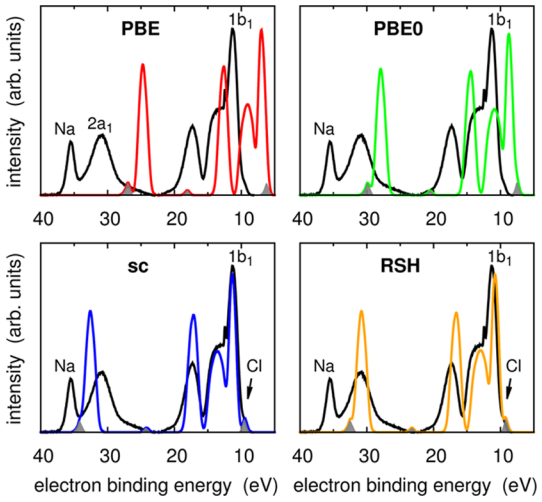

Figure 2. PE spectra of a 1 M aqueous NaCl solution computed with density functional approximations compared to the experimental spectrum of Figure 1. The gray area under the spectral features of sodium (2p) and chloride (3p) is the DOS projected on the maximally localized Wannier functions centered on the ionic sites. Theoretical spectra were aligned to the vacuum level (see text and Table SI).

To compute valence PE spectra, we first carried out simulations of a 1 M NaCl aqueous solution using the PBE0 hybrid functional.[20] The choice of this functional was motivated by its accuracy in the description of the structure of water and solutions of salts.[33,34] We calculated Kohn–Sham energies along PBE0 trajectories at the PBE,[29] PBE0, range-separated hybrid[32] (RSH), and self-consistent hybrid[31] (sc-hybrid) levels of theory. The latter functional and RSH include a fraction of exact exchange equal to the inverse macroscopic dieletric constant of water, determined self-consistently to be 0.6098. The attenuation parameter in the range-separated functional was set to 0.58 $bohr^{-1}$, i.e., the Thomas–Fermi screening length of water. Our simulations were conducted using the first-principles MD code *Qbox*;[35,36] subsequent electronic structure calculations employed the Quantum ESPRESSO[37] and WEST[38,39] codes. Further details are given in the Supporting Information (SI).

In pseudopotential calculations with periodic cells representing bulk samples, the position of the energy levels is defined up to an additive constant;[28,40] hence it is not straightforward to directly compare computed energies to experimental data, which are referred to the vacuum level.[12] To position the energy levels obtained in our periodic calculations with respect to vacuum, we computed the plane-average value of the electrostatic potential in the vacuum region of a water slab (liquid water in contact with a thick layer of vacuum).[41−43] Following ref 42, we simulated water slabs with classical potentials, and we determined the average values of the electrostatic potential outside the bulk region for all the density functionals employed in this work. Subtracting these values (SI) from the orbital energies of solutions obtained in bulk calculations, we determined the absolute single-particle energies referenced to vacuum.

Orbital energies computed in this way were used in calculations of the density of states (DOS), which we compared to the measurements reported in Figure 1, thus approximating electron BE with single-particle eigenvalues (see Figure 2). The positions of maxima of peaks in the spectra are reported in Table 1. Analysis of these data revealed that the PBE functional severely underestimates the absolute energies of water BE in the solution, in agreement with previous studies.[14,44] The BE of the $1b_1$ peak in the computed spectrum is shifted with respect to experiment by ~4.3 eV. The PBE0 hybrid functional brings a slight improvement, decreasing the discrepancy to ~2.6 eV. Compared to PBE and PBE0 results, the RSH and sc-hybrid functionals predict excellent PE spectra, deviating from experiment by only fractions of an eV. The RSH functional properly describes the BE of the water $2a_1$ state, while sc-hybrid slightly overbinds it. Interestingly, increasing the fraction of exact exchange in the density functional from zero (PBE) to ~60% (sc-hybrid) does not affect the relative BE of water $1b_2$ and $3a_1$ peaks with respect to the $1b_1$ peak (variation of <0.03 eV).

The relative position of the 3p level of Cl^- with respect to the water $1b_1$ peak is not reproduced even qualitatively at the PBE level of theory. The latter underestimates the separation of the 3p and $1b_1$ band maxima: 0.79 eV versus the experimental value of 1.71 eV. The PBE0 functional raises the 3p level of Cl^- above the VBM of water,[20] increasing the separation between the peaks to 1.23 eV. But it is only by using functionals where the mixing fraction of exact exchange is set to the inverse of the dielectric constant of water, i.e., RSH and sc-hybrid, that one obtains an almost quantitative agreement with experiment for the position of the Cl^- level. We note that these two functionals also yield the best orbital energies of Cl^- ions in the gas phase, superior to PBE0. (The differences between the computed and experimental[12] 3p BE of the gas-phase Cl^- ion are 3.5, 2.3, and 0.5 eV for PBE, PBE0, and RSH functionals, respectively. For the 2p level of Na^+, these differences are 11.3, 8.4, and 0.3 eV, respectively.)

The overall performance of the density functionals employed in this work was judged by the mean absolute percentage error (MAPE) reported in Figure S2. The range-separated and self-consistent functionals exhibit the best overall performance. With the MAPE of 7.2 and 6.5%, they both reproduce the distances between various peaks of the spectrum and yield accurate absolute energies (Figure 2). Compared to RSH, self-consistent hybrid predicts a $2a_1$ peak which is too bound (by ~1.7 eV) and the chloride peak a bit too high above the water VBM (by ~0.15 eV). (Results on single snapshots representing the liquid showed that the agreement with experiment would improve further if we used the experimental value of the dielectric constant of water (1.77[49]) in the definition of sc-hybrid and RSH functionals.) Note that

DOI: 10.1021/jacs.6b00225
J. Am. Chem. Soc. 2016, 138, 6912–6915

Table 1. Electron BE in PE Spectra of a 1 M NaCl Solution Computed Using DFT and Many-Body Perturbation Theory at the G_0W_0 Level[a]

method	2s (Na^+)	2p (Na^+)	$2a_1$	3s (Cl^-)	$1b_2$	$3a_1$	$1b_1$	3p (Cl^-)
PBE	54.94	26.90	24.71	18.06	12.63	9.03	6.99	6.20
PBE0	60.20	29.81	27.91	20.53	14.46	10.87	8.74	7.51
RSH	63.44	32.43	30.79	23.23	16.61	12.97	10.81	9.21
sc-hybrid	67.78	34.04	32.57	24.15	17.14	13.56	11.34	9.46
G_0W_0/PBE	64.08	32.99	28.82	20.14	15.97	12.26	9.89	8.76
G_0W_0/PBE0	66.83	34.28	29.91	21.32	16.85	13.21	10.73	9.43
G_0W_0/RSH	67.45	34.68	31.28	22.15	17.57	13.94	11.33	9.86
G_0W_0/sc-hybrid	68.44	35.06	31.69	22.36	17.58	13.91	11.41	9.89
experiment	68.0[b]	35.4[b]	30.90[c]	19.20–21[d]	17.409[e]	13.78[f]	11.31[e]	9.6[b,g]

[a]Absolute positions of all peaks with respect to vacuum are in eV. [b]Ref 12. [c]Ref 11. [d]Cl^- 3s peak is at 19.20 eV in LiCl solution,[45] 19.50 eV in $TiCl_3$ solution,[46] and at ~20–21 eV in $FeCl_3$[47] and $NiCl_2$[7] solutions. [e]Ref 48. [f]Average of $3a_1$H and $3a_1$L values in ref 48. [g]Ref 14.

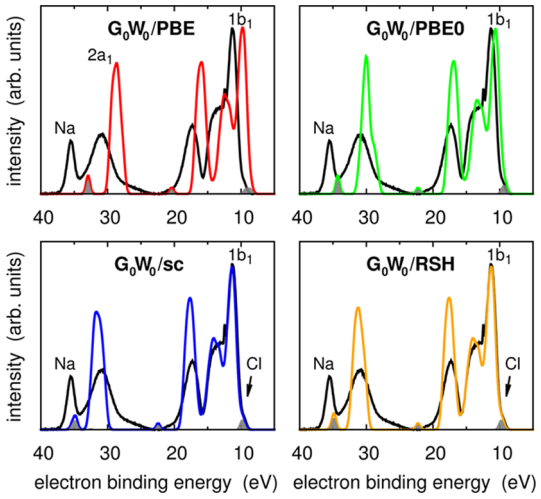

Figure 3. PE spectra of a 1 M aqueous NaCl solution computed using the G_0W_0 approximation starting from different sets of eigenfunctions and eigenvalues. Each theoretical spectrum is from a single snapshot representative of the entire trajectory. The spectra were aligned to the vacuum level (see text and SI). The gray area is projected DOS on Na and Cl atoms defined in Figure 2 caption.

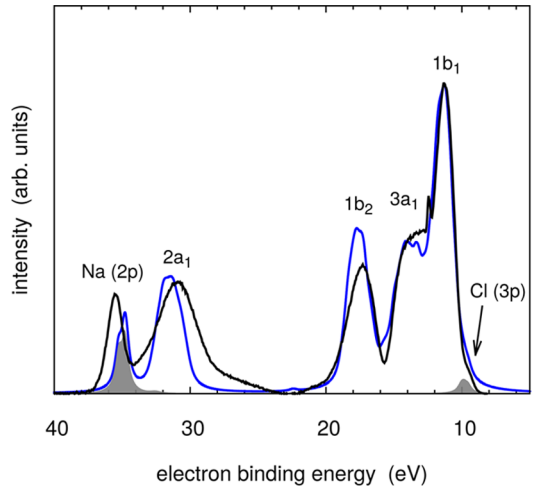

Figure 4. Experimental (black) and theoretical (blue) PE spectra of a 1 M aqueous solution of NaCl. Theoretical spectrum was computed using G_0W_0/sc-hybrid line widths and experimental photoionization cross sections as explained in the SI. Both spectra were normalized to the $1b_1$ peak of water. The gray area is projected DOS on Na and Cl atoms (see Figure 2 caption).

none of the functionals we used captured the energy of the sodium 2p level and reproduced the spacing of the $1b_2$, $3a_1$, and $1b_1$ bands of water with p-character.

To address these remaining issues, we turned to MBPT. Using the massively parallel WEST code,[39] we determined G_0W_0 corrections to eigenvalues obtained with PBE and hybrid functionals. We note that G_0W_0 excitation energies directly correspond to ionization energies.[50] In the case of pure water, we previously confirmed that the absolute energy of the highest occupied state computed within G_0W_0 agrees well with that computed using thermodynamic techniques and hence differences of free energies (see refs 23 and 25).

The results summarized in Figure 3 and Table 1 reveal a substantial, quantitative improvement when using MBPT: (i) The peaks of the spectrum belonging to water are in better agreement with experiment, in particular, the separation between the $1b_2$, $3a_1$, and $1b_1$ orbitals and the position of the $2a_1$ peak are greatly improved; (ii) the sodium 2p peak is separated from the water $2a_1$ peak for all functionals; the best agreement of the absolute position of the 2p level of sodium with experiment is 0.4 eV for the G_0W_0/sc-hybrid protocol; and (iii) the position of the Cl^- shoulder is improved, especially so when starting from hybrid functionals, indicating that a proper description of anions within MBPT requires accurate wave functions obtained from hybrid functionals. Note that the G_0W_0 corrections can have opposite signs for the same spectral features, depending on the error of the starting approximation: The $2a_1$ peak of water is blue-shifted when using PBE, PBE0, and RSH functionals, but red-shifted for the self-consistent hybrid.

Finally, we selected a computational protocol with the best overall performance for peak positions, G_0W_0/sc-hybrid, and computed the PE intensities using photoionization cross-sections and spectral line widths proportional to the imaginary part of the self-energy obtained within G_0W_0 (see SI). The computed spectrum, shown in Figure 4, is in very good agreement with our experimental result, including the relative intensities of $2a_1$, $3a_1$, and $1b_2$ peaks with respect to $1b_1$ peak and the sodium ion peak. The small discrepancy between the computed and measured spectra may be resolved if measured ionization cross sections and anisotropy parameters for the liquid water and solvated ions (see SI) become available.

In summary, we presented experimental and computed PE spectra of an aqueous solution of NaCl, which are in excellent agreement on an absolute energy scale for peak positions as well as for photoemission intensities. The agreement between theory and experiment is equally good for the energy levels of the isolated ions

DOI: 10.1021/jacs.6b00225
J. Am. Chem. Soc. 2016, 138, 6912–6915

and for ions in water. Comparison of our G_0W_0 results and those obtained with range-separated and self-consistent hybrids shows that these functionals yield semiquantitative agreement of PE spectra with experiment at a relatively modest computational cost, and they may be the method of choice, especially when analysis of trends and predictions of qualitative features are of interest. G_0W_0 calculations may then serve as benchmark and refinement of less computationally expensive hybrid calculations. We emphasize that accurate first-principles calculations of the electronic properties of solutions have long been out of reach due to the limited accuracy of existing DFT methods and the lack of adequate codes for MBPT calculations on large samples. Our results open the way to accurate, predictive calculations of the electronic properties of electrolytes, of interest to a variety of energy problems.

■ ASSOCIATED CONTENT

Supporting Information

The Supporting Information is available free of charge on the ACS Publications website at DOI: 10.1021/jacs.6b00225.

Experimental details and data (PDF)

■ AUTHOR INFORMATION

Corresponding Author

*gagalli@uchicago.edu

Notes

The authors declare no competing financial interest.

■ ACKNOWLEDGMENTS

We thank Dr. Federico Giberti for useful discussions. The work of M.G. and G.G. was supported by MICCoM as part of the Computational Materials Sciences Program funded by the U.S. Department of Energy (DOE), Office of Science, Basic Energy Sciences (BES), Materials Sciences and Engineering Division (5J-30161-0010A). Work by A.P.G. was supported by the U.S. Department of Energy, Office of Science, Basic Energy Sciences under Award DE-SC0008938 and by postdoctoral fellowship from the Natural Sciences and Engineering Research Council of Canada. Work of J.H.S. was supported by NSF under the NSF Center CHE-1305124. B.W. and R.S. were supported by the Deutsche Forschungsgemeinschaft (Collaborative Research Center 1109). The authors thank the HZB staff for their assistance during the beamtimes at BESSY II. An award of computer time was provided by the INCITE program. This research used resources of the Argonne Leadership Computing Facility, which is a DOE Office of Science User Facility supported under contract DE-AC02-06CH11357.

■ REFERENCES

(1) Nozik, A. J.; Memming, R. *J. Phys. Chem.* **1996**, *100*, 13061.
(2) Grätzel, M. *Nature* **2001**, *414*, 338.
(3) Goodenough, J. B. *Acc. Chem. Res.* **2013**, *46*, 1053.
(4) Cheng, J.; Sprik, M. *Phys. Chem. Chem. Phys.* **2012**, *14*, 11245.
(5) Bezanilla, F. *Nat. Rev. Mol. Cell Biol.* **2008**, *9*, 323.
(6) Finlayson-Pitts, B. J. *Phys. Chem. Chem. Phys.* **2009**, *11*, 7760.
(7) Seidel, R.; Thürmer, S.; Winter, B. *J. Phys. Chem. Lett.* **2011**, *2*, 633.
(8) Lange, K. M.; Aziz, E. F. *Chem. - Asian J.* **2013**, *8*, 318.
(9) Wilson, K. R.; Rude, B. S.; Catalano, T.; Schaller, R. D.; Tobin, J. G.; Co, D. T.; Saykally, R. J. *J. Phys. Chem. B* **2001**, *105*, 3346.
(10) Wilson, K. R.; Rude, B. S.; Smith, J.; Cappa, C.; Co, D. T.; Schaller, R. D.; Larsson, M.; Catalano, T.; Saykally, R. J. *Rev. Sci. Instrum.* **2004**, *75*, 725.
(11) Winter, B.; Weber, R.; Widdra, W.; Dittmar, M.; Faubel, M.; Hertel, I. V. *J. Phys. Chem. A* **2004**, *108*, 2625.
(12) Winter, B.; Weber, R.; Hertel, I. V.; Faubel, M.; Jungwirth, P.; Brown, E. C.; Bradforth, S. E. *J. Am. Chem. Soc.* **2005**, *127*, 7203.
(13) Winter, B.; Faubel, M. *Chem. Rev.* **2006**, *106*, 1176.
(14) Winter, B.; Faubel, M.; Hertel, I. V.; Pettenkofer, C.; Bradforth, S. E.; Jagoda-Cwiklik, B.; Cwiklik, L.; Jungwirth, P. *J. Am. Chem. Soc.* **2006**, *128*, 3864.
(15) Moens, J.; Seidel, R.; Geerlings, P.; Faubel, M.; Winter, B.; Blumberger, J. *J. Phys. Chem. B* **2010**, *114*, 9173.
(16) Seidel, R.; Thürmer, S.; Moens, J.; Geerlings, P.; Blumberger, J.; Winter, B. *J. Phys. Chem. B* **2011**, *115*, 11671.
(17) Schroeder, C. A.; Pluhařová, E.; Seidel, R.; Schroeder, W. P.; Faubel, M.; Slavíček, P.; Winter, B.; Jungwirth, P.; Bradforth, S. E. *J. Am. Chem. Soc.* **2015**, *137*, 201.
(18) Zhang, C.; Pham, T. A.; Gygi, F.; Galli, G. *J. Chem. Phys.* **2013**, *138*, 181102.
(19) Ge, L.; Bernasconi, L.; Hunt, P. *Phys. Chem. Chem. Phys.* **2013**, *15*, 13169.
(20) Gaiduk, A. P.; Zhang, C.; Gygi, F.; Galli, G. *Chem. Phys. Lett.* **2014**, *604*, 89.
(21) Bankura, A.; Santra, B.; DiStasio, R. A., Jr.; Swartz, C. W.; Klein, M. L.; Wu, X. *Mol. Phys.* **2015**, *113*, 2842.
(22) Swartz, C. W.; Wu, X. *Phys. Rev. Lett.* **2013**, *111*, 087801.
(23) Opalka, D.; Pham, T. A.; Sprik, M.; Galli, G. *J. Chem. Phys.* **2014**, *141*, 034501.
(24) Ghosh, D.; Roy, A.; Seidel, R.; Winter, B.; Bradforth, S.; Krylov, A. I. *J. Phys. Chem. B* **2012**, *116*, 7269.
(25) Opalka, D.; Pham, T. A.; Sprik, M.; Galli, G. *J. Phys. Chem. B* **2015**, *119*, 9651.
(26) Grell, G.; Bokarev, S. I.; Winter, B.; Seidel, R.; Aziz, E. F.; Aziz, S. G.; Kühn, O. *J. Chem. Phys.* **2015**, *143*, 074104.
(27) Adriaanse, C.; Cheng, J.; Chau, V.; Sulpizi, M.; VandeVondele, J.; Sprik, M. *J. Phys. Chem. Lett.* **2012**, *3*, 3411.
(28) Hunt, P.; Sprik, M. *ChemPhysChem* **2005**, *6*, 1805.
(29) Perdew, J. P.; Ernzerhof, M.; Burke, K. *J. Chem. Phys.* **1996**, *105*, 9982.
(30) Adamo, C.; Barone, V. *J. Chem. Phys.* **1999**, *110*, 6158.
(31) Skone, J. H.; Govoni, M.; Galli, G. *Phys. Rev. B* **2014**, *89*, 195112.
(32) Skone, J. H.; Govoni, M.; Galli, G. *Phys. Rev. B* **2016**, *93*, 235106.
(33) DiStasio, R. A., Jr.; Santra, B.; Li, Z.; Wu, X.; Car, R. *J. Chem. Phys.* **2014**, *141*, 084502.
(34) Gaiduk, A. P.; Gygi, F.; Galli, G. *J. Phys. Chem. Lett.* **2015**, *6*, 2902.
(35) *Qbox code* (version 1.56.2); UC Davis: Davis, CA; http://qboxcode.org/ (access date April 23, 2016).
(36) Gygi, F. *IBM J. Res. Dev.* **2008**, *52*, 137.
(37) Giannozzi, P.; et al. *J. Phys.: Condens. Matter* **2009**, *21*, 395502.
(38) Govoni, M.; Galli, G. *J. Chem. Theory Comput.* **2015**, *11*, 2680.
(39) *WEST code* (version 1.0.1); UChicago: Chicago, IL; http://west-code.org/ (access date April 23, 2016).
(40) Kleinman, L. *Phys. Rev. B* **1981**, *24*, 7412.
(41) Franciosi, A.; Van de Walle, C. G. *Surf. Sci. Rep.* **1996**, *25*, 1.
(42) Pham, T. A.; Zhang, C.; Schwegler, E.; Galli, G. *Phys. Rev. B* **2014**, *89*, 060202.
(43) Leung, K. *J. Phys. Chem. Lett.* **2010**, *1*, 496.
(44) Hunt, P.; Sprik, M.; Vuilleumier, R. *Chem. Phys. Lett.* **2003**, *376*, 68.
(45) Winter, B.; Aziz, E. F.; Ottosson, N.; Faubel, M.; Kosugi, N.; Hertel, I. V. *J. Am. Chem. Soc.* **2008**, *130*, 7130.
(46) Seidel, R.; Atak, K.; Thürmer, S.; Aziz, E. F.; Winter, B. *J. Phys. Chem. B* **2015**, *119*, 10607.
(47) Thürmer, S.; Seidel, R.; Eberhardt, W.; Bradforth, S. E.; Winter, B. *J. Am. Chem. Soc.* **2011**, *133*, 12528.
(48) Kurahashi, N.; Karashima, S.; Tang, Y.; Horio, T.; Abulimiti, B.; Suzuki, Y.-I.; Ogi, Y.; Oura, M.; Suzuki, T. *J. Chem. Phys.* **2014**, *140*, 174506.
(49) Sanchez-Valle, C.; Mantegazzi, D.; Bass, J. D.; Reusser, E. *J. Chem. Phys.* **2013**, *138*, 054505.
(50) Onida, G.; Reining, L.; Rubio, A. *Rev. Mod. Phys.* **2002**, *74*, 601.

DOI: 10.1021/jacs.6b00225
J. Am. Chem. Soc. 2016, 138, 6912−6915